

The Angular Transmittance Properties of Clouds

RICHARD T. HALL AND R. DOUGLAS RAWCLIFFE

The Aerospace Corporation, El Segundo, Calif. 90245

(Manuscript received 18 October 1971)

ABSTRACT

A series of experimental measurements of the visible light angular transmittance profiles of clouds is described. The results for single-layer overcast clouds were found to correlate well with standard hemispheric and narrow-angle pyrhelimetric transmittances. The resulting expression for the angular transmittance profile of an overcast cloud layer is

$$T(\theta) = A + B \sin^2\theta,$$

where

$$\left. \begin{aligned} A &= -0.0056 + 0.89T_n \\ B &= -0.028 + 1.09T_w \end{aligned} \right\}$$

and T is the transmittance measured for a field of view at the detector subtending a half angle θ centered about the sun or other light source, T_n the transmittance measured with a narrow-angle pyrhelimeter, and T_w the transmittance measured with a hemispheric pyrhelimeter.

1. Background and previous work

The scattering of light as it passes through a cloud has a major impact on the performance of an optical system operating with clouds in its optical path. In particular, the apparent transmittance of a cloud is dependent on the field of view of the sensor in the system. The optical engineer needs a fairly detailed knowledge of the transmission and scattering properties of clouds when designing an optical system to operate with visible light in the presence of clouds. While this subject has been treated extensively from a theoretical viewpoint (see, for example: Danielson *et al.*, 1969; Fritz, 1958; Hansen, 1969; Il'ich and Ivanov, 1965; Kattawar and Plass, 1968a, b; Plass and Kattawar, 1968a, b, c, d; Romanova, 1965; Twomey *et al.*, 1967), surprisingly few experimental measurements have been made by which the theories can be checked.

Haurwitz (1945, 1946, 1948) has correlated measurements of the total radiation from the sun and sky with cloud type and solar elevation angle. Unfortunately, these measurements give no information about the angular scattering distributions produced by the clouds since the measurements were made with a 2π field-of-view detector. Gibbons and co-workers (Gibbons, 1959; Gibbons *et al.*, 1961, 1962) have made studies of the effect of field of view on horizontal atmospheric transmission measurements. These measurements give the scattering properties of the atmosphere plus aerosols, haze, etc., but tell nothing about clouds. Arnulf *et al.* (1957) have made transmission measurements of haze and fog but unfortunately only with a detector with

a narrow angle field of view. The aircraft-based measurements of Neiburger (1949) and Griggs and Marggraf (Griggs and Marggraf, 1957; Marggraf and Griggs, 1969) of the transmission of solar radiation through clouds were again, unfortunately, made only with 2π field-of-view detectors.

Since no measurements were available of the visible light transmittance of clouds as a function of the field-of-view of the detector, an experimental measurement program was set up to obtain these data.

2. Instrumentation and experimental design

a. Experimental design

The site selected for the measurements was Eglin Air Force Base near Pensacola in northwestern Florida ($30^{\circ}20'N$, $86^{\circ}31'W$). This region of Florida experiences the fringes of the winter storms which sweep down across the United States from Canada and the artic. In the summer, cumulus clouds are prevalent due to the moisture-laden Gulf air.

In addition, there is at Eglin a well-equipped weather station with the standard meteorological instrumentation and a routinely operating cloud height radar, AN/TPQ-11. Personnel of Detachment 10 of the 6th Weather Wing operating this facility provided concurrent observations of meteorological conditions on a routine basis during the course of the experiment.

An additional experimental requirement was that simultaneous narrow- and wide-angle pyrhelimetric

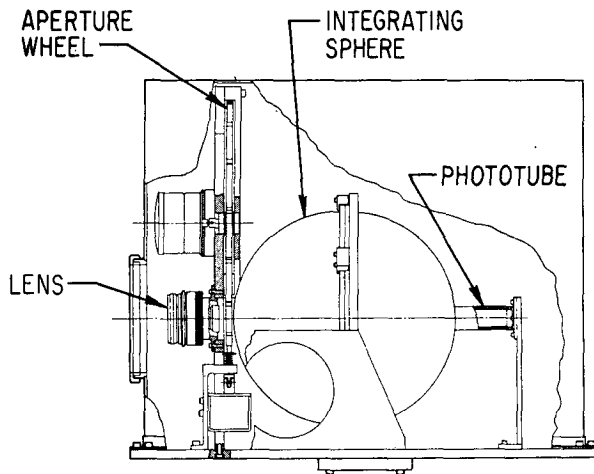


FIG. 1. Diagram of the cloud scattering instrument.

measurements be made¹. These measurements permit testing possible correlations of the experimental measurements with standard solar radiation measurements which are made on a routine basis at many stations around the world. The pyrheliometers were mounted adjacent to the scattering instrument.

b. Instrumentation

The basic components of the instrument designed to measure the angular scattering profiles of clouds, hereafter called the cloud scattering instrument, are a lens, a series of field stops, an integrating sphere, and a detector. The arrangement is shown in Fig. 1. The lens is a Nikkor 21-mm focal length, $f/4$ 35-mm camera lens. The field stops are thirteen holes drilled in a rotatable disc plus an opaque position. The hole sizes correspond to fields of view ranging from 0.95° to 32.2° half-angle. The integrating sphere is made from two 9-inch diameter plastic hemispheres with holes drilled at their "poles" for the entering and exiting light. The sphere is painted on the inside with 3M "White Velvet Coating" which is a 50-50 mixture of titanium dioxide and silicon dioxide. The detector is prevented from seeing direct radiation by a spider-mounted baffle on the optic axis 1.5 inches from the face of the detector. The detector is an RCA 7764 multiplier phototube with an S-11 response. This tube has its maximum response between 3900 and 5900 Å, and 50% sensitivity points at 3500 and 5700 Å (Radio Corporation of America, 1963).

The instrument is enclosed in a weather-tight box with an outer window of glass with a thin layer of evaporated chromium to act as a neutral density filter and heat reflector. Mounted on the same base plate and

¹ These instruments were lent to the Aerospace Corporation by the U. S. Army Electronics Proving Ground at Fort Huachuca, Ariz., through the efforts of Capt. Larry Johnson of Detachment 50 of the 6th Weather Wing at the Space and Missile Systems Organization (SAMSO).

bore-sighted with the cloud scattering instrument is an Eppley narrow-angle (2.85° half-angle field of view), normal incidence pyrheliometer. The pyrheliometer has a visual indicator of correct solar pointing which can be used when the sun is shining to adjust the alignment of the two instruments during operation.

The instrument and the narrow-angle pyrheliometer are mounted on a conventional astronomical telescope clock drive whose polar axis was carefully aligned to true north. An appropriate declination adjustment of the instruments permitted correct tracking of the sun with the sun centered in the fields of view of the apertures. Electrical and signal connections are made through a set of slip rings mounted on the polar axle to prevent wind up of the cabling by the rotation of the drive.

The instrument was placed on a wooden platform on the roof of a hangar at Eglin Air Force Base approximately 50 ft above the ground. Fig. 2 shows the instrument in place. The Eppley wide-angle (2π field of view) pyrheliometer was placed in an unshaded location on the roof of a small penthouse and can be seen above and to the right of the instrument. The entrance aperture of the narrow-angle pyrheliometer can be seen behind the instrument box.

The power and signal cabling was run ~ 200 ft to the Weather Operations room on the floor of the hangar where the recording electronics were housed. Because of the long cable run, preamplifiers were included in the weather-proof box.

The operation of the experiment was as follows. A 24-hr timer turned the electronics on before sunrise and off after sunset. A set of data was taken automatically every 10 min during the intervening time. The instrument sequenced through the thirteen apertures from smallest to largest, stopping 1-2 sec at each aperture to allow recording of the signal. After sequencing through the thirteen apertures the instrument turned itself off at the opaque position. A zero (opaque) reading was taken at the start and end of each sequence. After cycling through the apertures, the instrument recorded the signals from the two pyrheliometers. Thermistors located in the cloud instrument and each of the pyrheliometers were then sampled. Finally the minute, hour and day were recorded from a digital clock/calendar. The entire cycle took about a minute, after which the electronics went into standby until another 10 min elapsed.

The pyrheliometric measurements were made with two standard Eppley pyrheliometers, a 50-junction hemispheric pyrheliometer and a Model 15 normal-incidence pyrheliometer (U. S. Weather Bureau, 1962). The cloud height radar in operation at Eglin Air Force Base was a model AN/TPQ-11 Radar Cloud Detecting Set operating in the K_A frequency band (33-36 GHz) (Boucher and Wexler, 1965). The facsimile chart recordings from this instrument were delivered to Aerospace Corporation personnel who interpreted them.

Kantor (1968) has analyzed the detection capabilities of the AN/TPQ-11 radar and has found that only 62% of visually-observed overcast clouds were detected by the radar. Because of this deficiency, it was necessary to use, in addition, standard visual cloud assessments to determine the existing cloud cover at the time of the measurements. These observations were made hourly except when rapidly changing conditions warranted more frequent observations. The supplemental coded data included the synoptic coded observations of low, middle and high clouds (C_L, C_M, C_H) (U. S. Weather Bureau, Air Force, Navy, 1966). These were recorded every 3 hr. These synoptic measurements were used to identify the clouds present during our measurements. Identifications between the synoptic observations were made by interpolating between the bracketing observations using the remarks recorded by the observer as to advancing or receding clouds. Standard meteorological observational data were supplied by the personnel at Eglin Air Force Base on WBAN Form 10 which includes the following data used in this experiment: time, sky condition, horizontal visibility, temperature and dew point, total sky cover, remarks and supplemental coded data.

c. Calibration

The calibration of the cloud scattering instrument entailed several steps. All the measurements were made in a darkroom using a small but very bright tungsten coil lamp mounted in the same horizontal plane of the cloud scattering instrument and about 20 ft away. A slight adjustment in the focus of the lens of the instrument was made to correct for the non-parallelism of the light from 20 ft.

The normalization factors between the apertures were determined by measuring the on-axis signal for each aperture and normalizing to the smallest aperture (1°). The effective angular field of view of each aperture was determined as follows. With no limiting aperture the intensity is given by a $\cos^4\theta$ angular distribution². The signal was measured at a number of angles on both sides of the optic axis (in a horizontal plane only). The two points at which the signal dropped to 50% of the above-mentioned $\cos^4\theta$ value were averaged to give the effective field of view of a given aperture. The areas under these curves of angular response were measured with a planimeter to determine the solid angle factor for each aperture, i.e., a correction factor for the vignetting of the field of view at off-axis positions. An absolute sensitivity calibration was not attempted because uncertainties in the value of the spectral integral of the product of the solar irradiance and the instrumental response function would have prevented its meaningful use. Instead, as discussed below, the response was

² The $\cos^4\theta$ represents the falloff of intensity of off-axis rays due to geometric factors. See, for example, Jenkins and White, *Fundamentals of Optics*, Chap. 7.

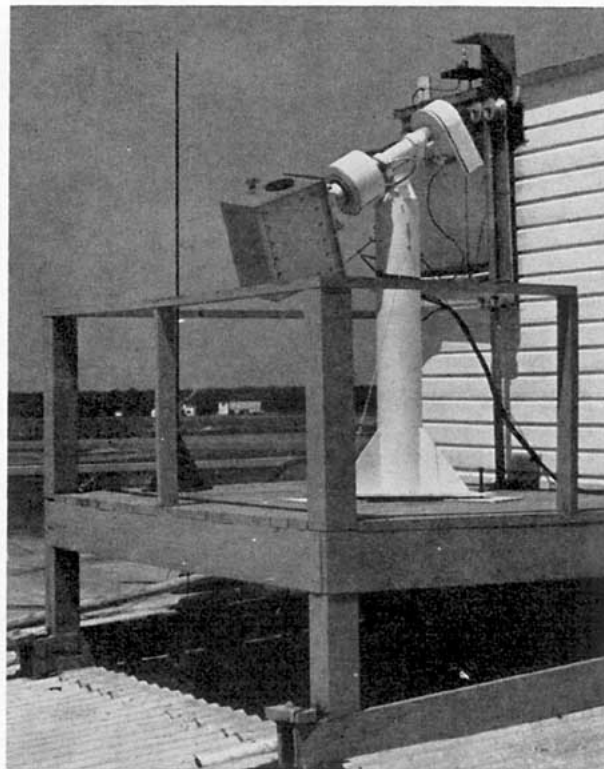


FIG. 2. Experimental set-up on the hangar roof showing the cloud scattering instrument and the two pyrhemometers.

normalized against the transmittance for a very clear day.

The conversion-calibration factor (langley per volt) for each of the pyrhemometers is given by the Epply Company with their instruments. However, the signal received at the recorder was also affected by the gains of the preamplifiers and by losses in the required long cables. It was impractical to calibrate the entire pyrhemometer-preamplifier-signal cable assembly as installed in Florida. Again, the absolute sensitivities of these instruments were estimated by normalizing against the calculated transmittance on a very clear day.

Several crystal-clear days with very high reported horizontal visibility occurred in the early period of the experiment. The calculated transmittance of a Rayleigh atmosphere in the spectral region passed by the glass bulb of the pyrhemometers is 0.904 and the calculated transmittance³ of a turbid atmosphere is 0.718. Since the atmospheric conditions on these crystal-clear days seemed to be clearer than those described by Elterman for his "turbid" atmosphere, the simple Rayleigh

³ The calculated transmissions are based on Elterman's atmospheric attenuation model as given in *Handbook of Geophysics and Space Environments*, Air Force Cambridge Research Laboratories (McGraw-Hill, 1965, Chap. 7). The spectral range was considered to be that passed by the glass window or envelope of the pyrhemometers; namely 0.35–2.5 μ . The sun with a spectral distribution as given in Chap. 16 of the *Handbook* was used for the radiation source.

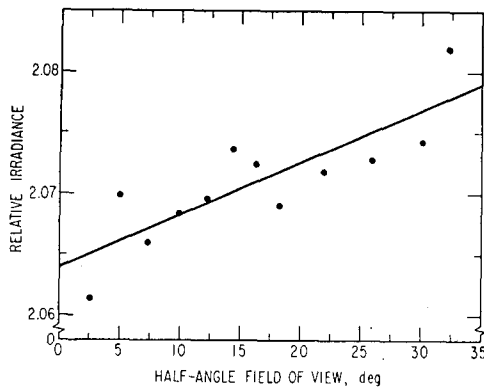


FIG. 3. Plot of the relative irradiance for 1205 local time 1 March 1968. This data set was used as the "clear sky" reference.

atmospheric transmittance of 0.90 was adopted for the pyr heliometric readings on these days. Using this value of the transmittance, the calibration factors of the pyr heliometers were calculated. The absolute accuracy of the pyr heliometric measurements does not affect the shapes of the angular transmittance profiles which are more significant to this study than their absolute magnitudes.

3. Experimental operation and data sample

a. Period of experiment

The experiment was operated between 9 February and 18 October 1968. Because of equipment malfunctions data were obtained only for the periods 9 February through 3 April, 5–9 April, 17 April through 22 May, 12 June through 21 July, 28 August through 4 October, and 16–18 October. (The data for 15–22 May were lost in the mails.) The narrow-angle pyr heliometer was inoperative for the period 12 June through 21 July. The data for the period 28 August to the end of the experiment are considered unreliable because of a belatedly discovered possible misfocus and f /stop change. Reliable, complete data are available, therefore, for only 88 days between 9 February and 14 May. In addition, incomplete data (narrow-angle pyr heliometer inoperative) are available for the 40-day period between 12 June and 21 July.

b. Data sample

During the 88-day period for which complete data are available, a total of 3296 measurements were made with the sun higher than 35° above the horizon. Of these 3296 measurements, 530 were made during completely clear skies (0/10 cloud cover) and 1200 during completely overcast skies (10/10 cloud cover). The 1566 measurements made during periods of broken or scattered clouds were not used for further analysis because of the uncertain location of holes in the clouds with respect to the sun's position. In addition, measurements of overcast clouds made when more than one

layer of clouds was reported were also not used for further analysis. This was because of uncertainties about breaks in the individual layers. This left a sample of 530 measurements during completely clear skies and 398 measurements made during single-layer, completely overcast skies. Of the 398 overcast measurements, 64 were discarded because of various problems with the data. Table 1 gives the breakdown of the measurements upon which the analysis was based.

4. Data reduction

The instrumental data and other observational information were coded into computer-compatible form. These data were used to compute mean relative radiances and irradiances, the wide- and narrow-angle pyr heliometric transmittances, the relative humidity, and the solar elevation angle. Standard formulas for the sun-earth geometry (Robinson, 1966) were used to compute the pyr heliometric transmittances and the solar elevation angle.

A small tilt ($\sim 3^\circ$ to the WNW) of the wide-angle pyr heliometer occurred shortly after its installation. The error ($\sim 5\%$) introduced by this tilt was removed by suitable geometric corrections in the transmittance formulas.

The relative irradiances derived by the computer analysis were converted into transmittances by the following technique. Since there was no way to derive absolute transmittances from the relative irradiances, an alternative was to derive the transmittances relative to a clear sky. The transmittances could be determined from the relative irradiances by dividing these irradiances by the relative irradiance of a clear sky. The highest irradiance values were recorded under clear sky conditions on 1 March 1968 at 1205 local time. These data were chosen as the "clear sky" reference.⁴ No

TABLE 1. Number of complete measurements of single-layer completely overcast cloud cover by cloud type.

Cloud type	Name	Number of measurements
Low clouds		
$C_L = 3$	Cumulonimbus	3
$C_L = 4$	Stratocumulus cumulogenitus	5
$C_L = 5$	Stratocumulus	34
$C_L = 6$	Stratus	127
Middle clouds		
$C_M = 1$	Altostratus	5
$C_M = 3$	Alto cumulus translucidus	5
$C_M = 7$	Alto cumulus opacus	17
High clouds		
$C_H = 1$	Cirrus fibratus	5
$C_H = 7$	Cirrostratus	133
Incomplete data or unknown cloud type		64

⁴ The meteorological condition at this time were: 14 mi horizontal visibility, 47F air temperature with 22% relative humidity, and a 4-kt wind blowing out of the northwest. The weather map for the day showed a high pressure system centered off the Louisiana coast.

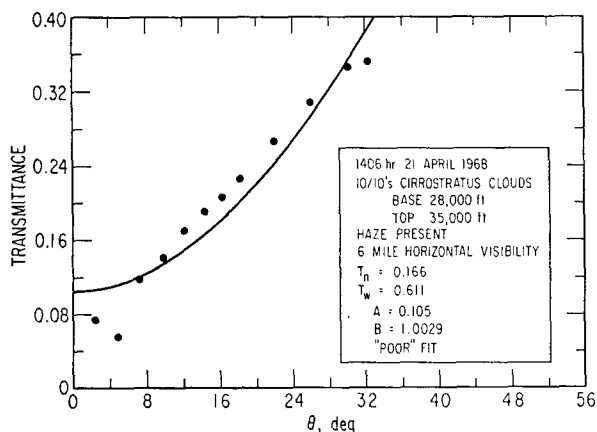
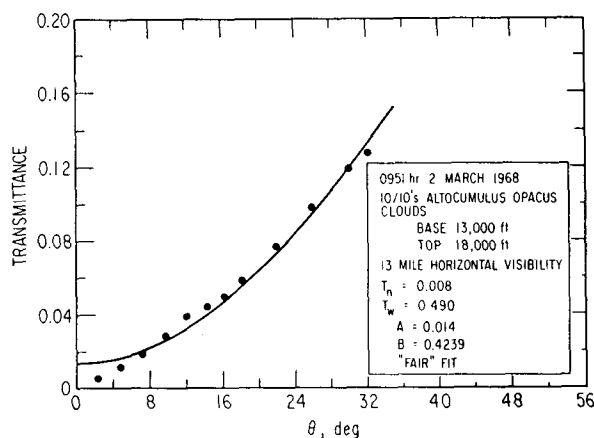
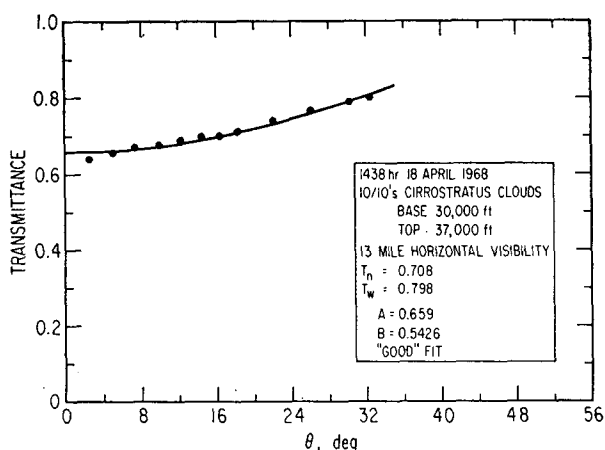
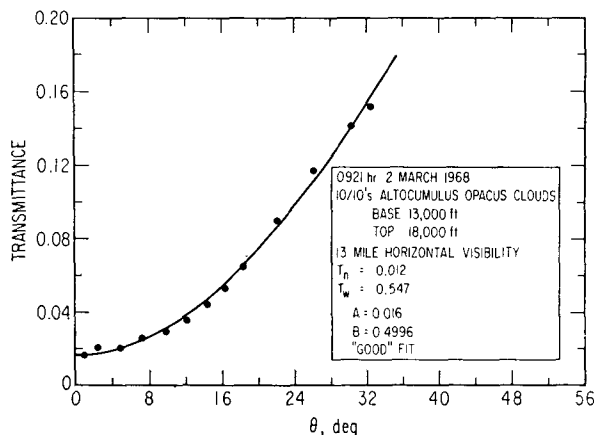
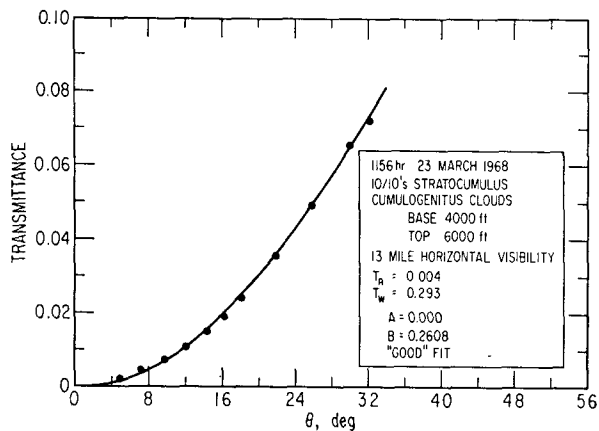


FIG. 4. Sample data plots showing examples of qualities of fit to Eq. (1). The dots are the experimental transmittances, the solid line the least-squares fitted curve of (1). Examples of good, fair and poor results are shown.

clouds were reported for the entire day until late in the afternoon when some cirrus clouds appeared in the southwest portion of the sky. The pyrheliometric data⁵ were $0.87 T_w$ and $0.90 T_n$. The relative irradiance profile is shown in Fig. 3, together with a linear least-squares fit to these data. The figure shows that the circumsolar sky contributes less than 1% to the total reading at full aperture.

⁵ The obviously impossible condition that the narrow-angle transmittance is greater than the wide-angle transmittance is probably a reflection of the absolute accuracies of the measurements, i.e., $\pm 1-3\%$.

After converting the relative irradiance data to transmittances, each set of data was fitted to the expression

$$T(\theta) = A + B \sin^2 \theta, \quad (1)$$

where T is the transmittance and θ the half-angle of the field of view. The angular factor arises from the geometric factor in the solid angle formulation and the $\cos \theta$ weighting for diffuse light. The coefficient A is a measure of the direct transmittance and B of the diffuse. The agreement of the data with this expression was, in general, good. On an entirely subjective basis, of the

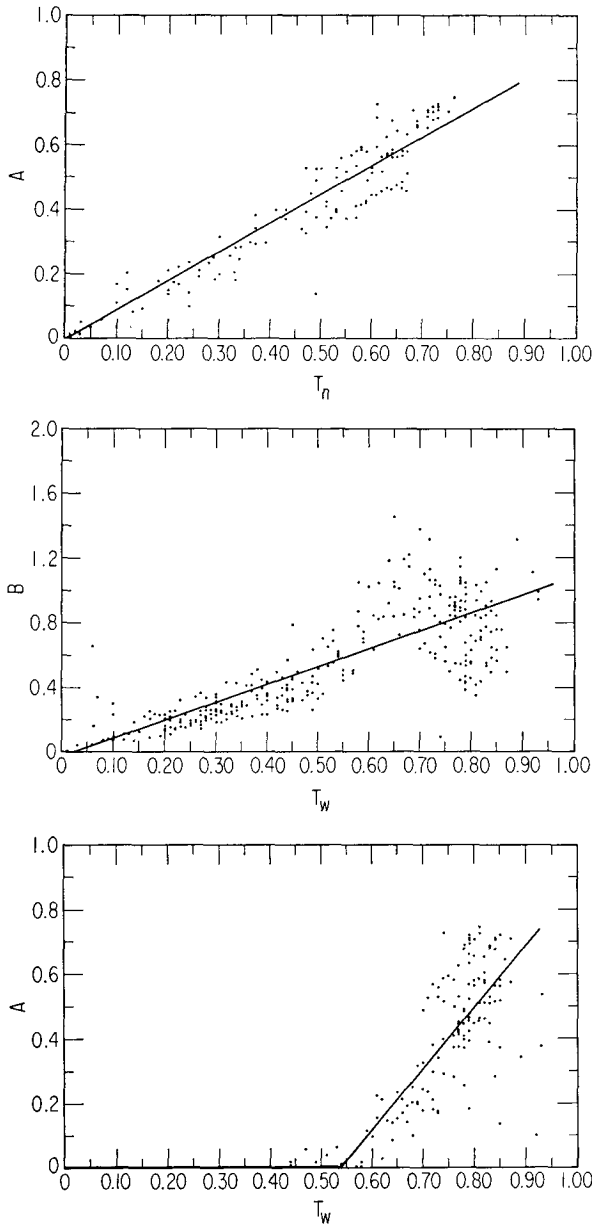


FIG. 5. Scatter diagrams showing correlations of measured transmittances with the constants of Eq. (1): T_n vs A (a), T_w vs B (b), T_w vs A (c).

334 sets of data of single-layer overcast clouds, 202 gave "good" agreement with the expression, 111 gave "fair" agreement, and only 21 gave "poor." Sample plots of "good," "fair," and "poor" agreement are shown in Figs. 4a-e.

With the coefficients A and B from (1) as descriptors of the transmittance profiles, correlations of these coefficients with routinely measured actinometric quantities were tested. The four combinations of A and B with T_w and T_n were used in this study.

Linear least-squares fits of these data and their correlation coefficients were calculated. The "poor" data

TABLE 2. Least-squares fitted relationships between T_n , T_w , A and B .

T_n vs A :	$A = -0.0056 + 0.89 T_n$ [correlation coefficient, 0.98]
T_w vs A :	$A = -0.0026 + 0.0126 T_w (T_w < 0.54)$ [correlation coefficient, 0.24] $A = -1.0427 + 1.92 T_w (T_w \geq 0.54)$ [correlation coefficient, 0.76]
T_w vs B :	$B = -0.0281 + 1.09 T_w$ [correlation coefficient, 0.77]
T_w vs T_n :	$T_n = -0.00417 + 0.029 T_w (T_w < 0.54)$ [correlation coefficient, 0.45] $T_n = -1.190 + 2.19 T_w (T_w \geq 0.54)$ [correlation coefficient, 0.84]

were omitted from these calculations. Plots of the successful correlations are given in Figs. 5a-c. Fig. 5a shows a linear correlation between T_n and A with an intercept at the origin. This is reasonable in view of the fact that both are measures of the direct sunlight. A linear correlation between T_w and B with an intercept at the origin is again indicated in Fig. 5b, although the scatter is fairly great at large values of T_w . This correlation is also reasonable in view of the fact that both quantities are measures of the diffuse radiation.

No simple correlation between T_n and B was found as would be expected. Fig. 5c illustrates a more complex situation. A linear correlation seems to exist between T_w and A but with a non-zero intercept. It would seem that a threshold value of T_w must be exceeded before A has a non-zero value. This supports the theoretical interpretation of Twomey *et al.* (1967) that the angular distribution of the transmittance is practically constant if the optical thickness of the cloud exceeds 10. This is reasonable from the observation that the sun can be seen through the clouds only for a range of transparency of the clouds. For more opaque clouds no direct sunlight can be seen. The calculation of T_w vs A requires that the threshold point be determined first. This point was found by using only those values in the least-squares calculations whose T_w coordinate was above some arbitrary value. The threshold point was

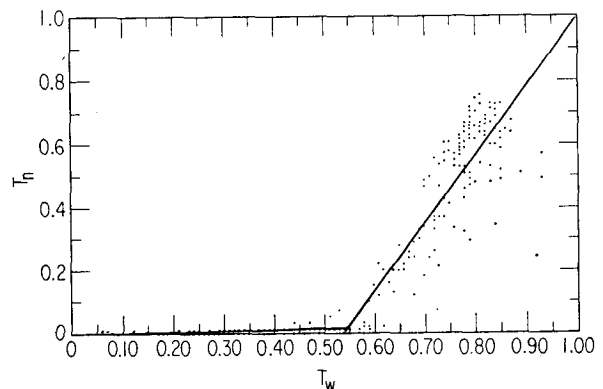


FIG. 6. Scatter diagram showing correlation of T_w with T_n .

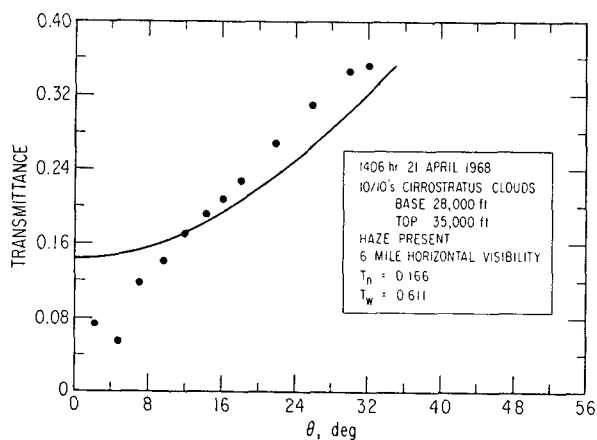
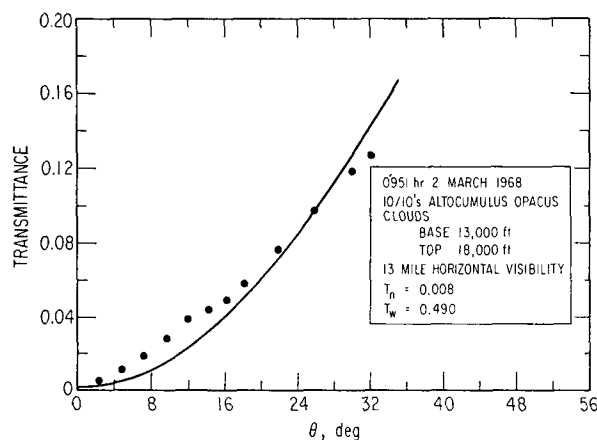
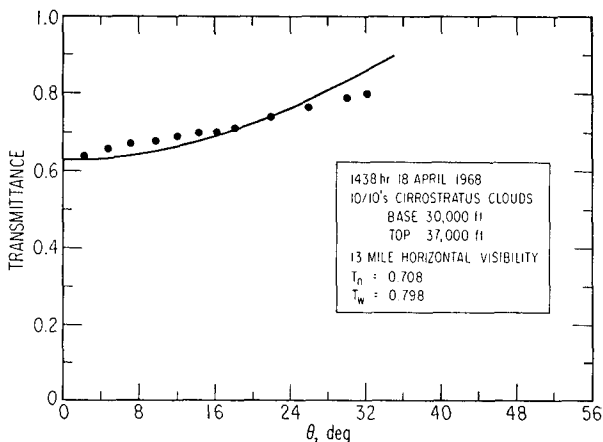
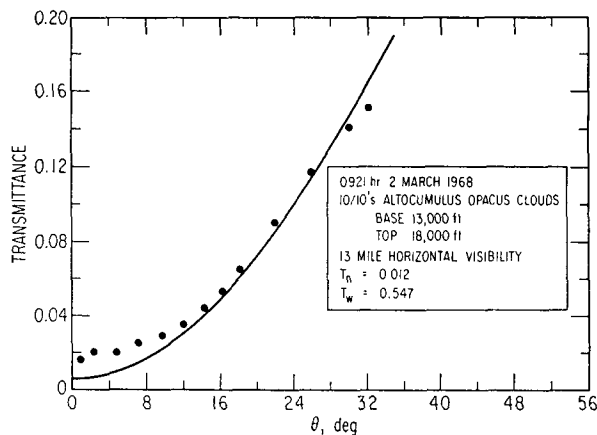
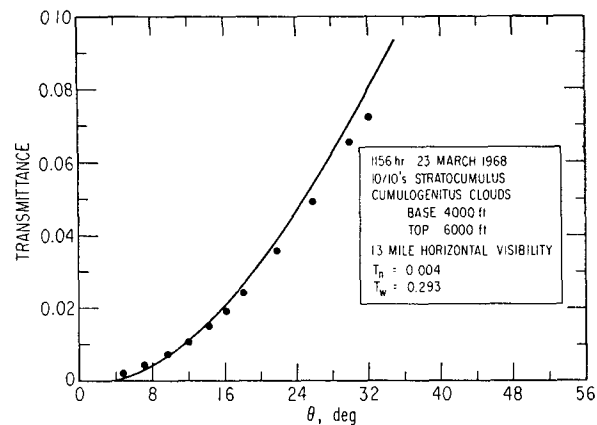


FIG. 7. Sample data plots of transmittances vs field of view showing accuracy of model. The dots are the experimental transmittances; the solid line is calculated from Eq. (2) using experimental values of T_n and T_w .

defined when the T_w cutoff most nearly equalled the T_w -axis intercept. The threshold determined by this method was 0.54. The results of the linear least-squares calculations are plotted in Figs. 5a-c and the regression equations given in Table 2.

An additional correlation between T_w and T_n was tested. The results were qualitatively similar to those for the correlation between T_w and A . The least-squares fit with a T_w threshold of 0.54 gave the straight line shown in Fig. 6 and the results summarized in Table 2.

No correlation between the irradiance measurements

and cloud type was found. This is probably due to the great variability in cloud characteristics within a cloud type. The same cloud type can exist over a wide range of thicknesses and opacities.

Because of the good correlation between T_n and A and between T_w and B , it would appear that a reasonable model of the angular transmittance characteristics of clouds has been found which can be quantitatively calculated from two routine meteorological observations. Combining the results tabulated in Table 2 with Eq. (1) results in the following formula for the visible

light angular transmittance of a cloud relative to that of the clear sky as a function of the narrow- and wide-angle pyrhelometric transmittance:

$$T = -0.0056 + 0.89T_n + (-0.028 + 1.09T_w) \sin^2\theta. \quad (2)$$

The formula is valid at least for $\theta \leq 35^\circ$. For larger values of θ , an extrapolation of unknown accuracy is assumed.

How well this model will predict the angular transmittance profiles is shown in Figs. 7a-e. The data are the same as used in Fig. 4. The lines in the figures are calculated from (2), while the points are the observed data. The agreement of the calculated lines with the observed points is quite satisfactory. An estimate of the accuracy of a calculated transmittance is ± 0.01 or $\pm 10\%$, whichever is greater.

6. Interpretation and application

a. Interpretation

The success of the angular transmittance model developed here is a validation of the idea that the transmission of light through the atmosphere has two components, one direct and one scattered, and that these components are separable. The relative magnitudes of the two components vary with the characteristics of the scattering media in the light beam. The direct component is important only when the wide-angle transmittance of the scattering media is greater than roughly 0.50.

Diffuse radiation is usually taken to mean an intensity decrease with the cosine of the angle to the normal of the surface from which the radiation emerges. Such a surface appears equally bright from all directions because this cosine dependence just compensates for the foreshortening of the surface as seen by the observer. The diffuse component of T , $B \sin^2\theta$, which was calculated from this experiment would have been simpler to explain if the measurements could have been made by observing at the zenith so that the vector to the sun would have been perpendicular to the cloud layer. Then θ would have been the ray angle from the cloud normal. However, the minimum solar zenith angle during the experiment was about 12° and measurements were necessary at still larger zenith angles (to 55°) to obtain a reasonable data sample. Because a diffuse surface appears equally bright in all directions, the readings obtained for the diffuse components are still properly made. Note, however, that for non-zero solar zenith angles, the path length of the radiation through the cloud increases and the transmittance decreases. This is borne out qualitatively by the diurnal plots of T_w (denoted PPT) in an analysis of actinometric data for the Soviet Union (Hall, 1967a, b).

It should be possible to relate T_w and T_n directly to A and B , as follows. Indeed $T = T_w$ for $\theta = 90^\circ$ and $T = T_n$ for $\theta = 2.85^\circ$. If we use these relations to evalu-

ate A and B we find that

$$T \approx T_n + (T_w - T_n) \sin^2\theta.$$

These values of A and B do not correlate with the experimental data as well as those deduced above. Possible partial explanations for this discrepancy are as follows:

1) The cloud scattering instrument measures in the spectral band from about $0.35\text{--}0.57 \mu$ with an S-11 photomultiplier response. The pyrhelometers are thermal detectors which respond to all wavelengths transmitted by the atmosphere and by their glass envelopes or windows, i.e., from about $0.35\text{--}2.5 \mu$. The scattering properties of the cloud droplets are wavelength dependent.

2) The corrections for atmospheric absorption used in the normalizations are not the same for the two types of instruments.

3) The model was derived only for $\theta \leq 35^\circ$. An extrapolation of the model to $\theta = 90^\circ$ is of unknown accuracy.

b. Application

The model derived for the angular transmittance profile of visible solar radiation through clouds has several limitations on its validity and applicability. The primary limitation is that the model is valid only for single, overcast cloud layers. Multiple cloud layers cannot be treated for the simple reason that the light impinging on the second layer after emerging from the first layer no longer can be considered to be collimated. Rather it has a scattered component which will diffusely illuminate the second layer, thereby grossly deviating from the conditions of the model.

Likewise the model is inapplicable for broken clouds even with the source behind one of the clouds. The direct component is affected by the presence of broken clouds to the same extent as it was for an overcast layer. However, the scattered component will be grossly changed because of the non-uniform scattering medium. The change can be either to increase or decrease the apparent scattered component. The increase could result from strong reflections from the sides of the clouds into the field of view of the sensor. A decrease might result from a fortuitous arrangement of the clouds so as to preferentially scatter the beam away from the sensor with little or no scattering back into the beam. Such a case might be a single small cloud directly in front of the source with no other clouds in the sky.

A further limitation is that the model is applicable only to collimated light. Diverging or converging light might deviate wildly from the results predicted by the model. This aspect of the model is subject to experimental verification albeit with considerable difficulty.

What has been developed here is a model which describes the angular transmittance characteristics of collimated visible light through a single, overcast layer

of clouds. The model gives satisfactory agreement with experimental observations. The model should be of general use in the evaluation and prediction of the performance of visible light optical systems in the presence of clouds. It should serve as a useful stepping-off point for the development of models of more complex situations such as broken clouds or multiple cloud layers. It should also serve as a useful test for theoretical models of collimated light incident on an infinite scattering layer.

Acknowledgments. The authors would like to thank Mr. Tom Mott for all his assistance in setting up and running the experiment; Mr. Ronald Williams for his work in designing the electronics and data recording systems; Major Jack Coblenz, Mr. Brent Walker, and all the staff of Detachment 10 of the 6th Weather Wing for their aid, assistance and hospitality during the course of the experiment; and finally Mrs. Gwen Boyd and her staff of mathematical aides for their untiring efforts in the transcription of the data onto computer coding sheets. This work was performed under Air Force Contract AF04-(695)-1001.

REFERENCES

- Arnulf, A., J. Bricard, E. Curé and C. Vêret, 1957: Transmission by haze and fog in the spectral region 0.35 to 10 microns. *J. Opt. Soc. Amer.*, **47**, 491-498.
- Boucher, R. J., and R. A. Wexler, 1965: Preliminary operational application techniques for AN/TPQ-11. Rept. AWS TR-180, United Aircraft Corp. Systems Center. (Available from the Defense Documentation Center, AD-609305.)
- Danielson, R. E., D. R. Moore and H. C. van de Hulst, 1969: The transfer of visible radiation through clouds. *J. Atmos. Sci.*, **26**, 1078-1087.
- Fritz, S., 1958: Absorption and scattering of solar energy in clouds of "large water drops"—II. *J. Meteor.*, **15**, 51-58.
- Gibbons, M. G., 1959: Experimental study of the effect of field of view on transmission measurements. *J. Opt. Soc. Amer.*, **49**, 702-709.
- , F. I. Laughridge, J. R. Nichols and N. A. Krause, 1962: Transmission and scattering properties of a Nevada desert atmosphere under cloudy conditions. *J. Opt. Soc. Amer.*, **52**, 38-43.
- , J. R. Nichols, F. I. Laughridge and R. L. Rudkin, 1961: Transmission and scattering properties of a Nevada Desert atmosphere. *J. Opt. Soc. Amer.*, **51**, 633-640.
- Griggs, M., and W. A. Marggraf, 1967: Measurement of cloud reflectance properties and the atmospheric attenuation of solar and infrared energy. Rept. General Dynamics/Convair AFCRL-68-0003. (Available from Defense Documentation Center, AD-666936.)
- Hall, R. T., 1967a: Soviet actinometric data, Vol. I: Analysis of data. Rept. TR-1001(2192)-1, Vol. I, Aerospace Corp. (Available from the Defense Documentation Center, AD-814999.)
- , 1967b: Soviet actinometric data, Vol. II: Compilation of Data. Rept. TR-1001(2129)-1, Vol. II, Aerospace Corp. (Available from the Defense Documentation Center, AD-815249.)
- Hansen, J. E., 1969: Exact and approximate solutions for multiple scattering by cloudy and hazy planetary atmospheres. *J. Atmos. Sci.*, **26**, 478-487.
- Haurwitz, B., 1945: Insolation in relation to cloudiness and cloud density. *J. Meteor.*, **2**, 154-166.
- , 1946: Insolation in relation to cloud type. *J. Meteor.*, **3**, 123-124.
- , 1948: Insolation in relation to cloud type. *J. Meteor.*, **5**, 110-113.
- Il'ich, G. K., and A. P. Ivanov, 1965: Diffuse reflection of light from the optically thick layers of scattering media. *Izv. Atmos. Oceanic Phys.*, **1**, 343-347.
- Kantor, A. J., 1968: Cloud detection capability of operational AN/TPQ-11 radar sets during 1966-1967. Air Force Cambridge Research Lab., Rept. AFCRL-68-0269. (Available from Defense Documentation Center, AD-671484.)
- Kattawar, G. W., and G. N. Plass, 1968a: Influence of particle size distribution on reflected and transmitted light from clouds. *Appl. Opt.*, **7**, 869-878.
- , and —, 1968b: Radiance and polarization of multiple scattered light from haze and clouds. *Appl. Opt.*, **7**, 1519-1527.
- Marggraf, W. A., and M. Griggs, 1969: Aircraft measurements and calculations of the total downward flux of solar radiation as a function of altitude. *J. Atmos. Sci.*, **26**, 469-477.
- Neiburger, M., 1949: Reflection, absorption, and transmission of insolation by stratus cloud. *J. Meteor.*, **6**, 98-104.
- Plass, G. N., and G. W. Kattawar, 1968a: Influence of single scattering albedo on reflected and transmitted light from clouds. *Appl. Opt.*, **7**, 361-367.
- , and —, 1968b: Monte Carlo calculations of light scattering clouds. *Appl. Opt.*, **7**, 415-419.
- , and —, 1968c: Radiant intensity of light scattered from clouds. *Appl. Opt.*, **7**, 699-704.
- , and —, 1968d: Calculations of reflected and transmitted radiance for the earth's atmosphere. *Appl. Opt.*, **7**, 1129-1135.
- Radio Corporation of America, 1963: RCA phototubes and photocells. Lancaster, Pa., 171-172.
- Robinson, N., 1966: *Solar Radiation*. Amsterdam, Elsevier Publ. Co., 29-46.
- Romanova, L. M., 1965: Limiting cases of the path distribution function of photons emerging from a thick light-scattering layer. *Izv. Atmos. Oceanic Phys.*, **1**, 348-351.
- Twomey, S., H. Jacobowitz and H. B. Howell, 1967: Light scattering by cloud layers. *J. Atmos. Sci.*, **24**, 70-79.
- U. S. Weather Bureau, 1962: *Manual of Radiation Observations*. Washington D. C., Govt. Printing Office, 1-61.
- , Air Force, Navy (WBAN), 1966: *Manual of Surface Observations, Circular N*, 7th ed. (revised). Washington D. C., Govt. Printing Office, 1-22 to 1-30, 3-10, 7-17, 9-1 to 9-7, 10-1 to 10-10.